Chapter 11
Magnetic Nanoparticle-Based Hyperthermia for Cancer Treatment: Factors Affecting Heat Generation Efficiency

Yasir Javed, Khuram Ali, and Yasir Jamil

11.1 Introduction

The importance of nanotechnology-based medicines, i.e., nanomedicines, has been increasing greatly in recent years [1]. Owing to the familiar side effects of anticancer drugs, medicines with high efficacy and selectivity were indispensable [2]. The problem of inconsistent proliferation of drugs at tumor sites while causing comparatively less damage to normal tissues can be resolved with nanoparticles. Nanoparticles can release drugs by the action of an external signal, pH values, or physiological conditions inside tissues or cells [3]. In addition, there are great economic benefits associated with the use of nanotechnology in cancer treatment. In general, nanotechnology is poised to have a ground-breaking impact on cancer diagnosis and therapy [4, 5].

Noninvasive, early-stage cancer detection is a major challenge and a precondition for its treatment. It is also important to secure the greatest therapeutic advantages. In cancer treatment, cell-specific and localized drug delivery is a crucial challenge [6]. A powerful fight against cancer requires efficient attacks on cancer cells while preserving normal cells from unnecessary drug loadings [7]. Conversely, the majority of anticancer drugs are developed with a view to simply killing cancer cells and distributing drugs in healthy organs or tissues, without regard for the concomitant severe side effects in normal tissues [8]. Furthermore, for fast elimination and broad distribution from healthy/nontargeted organs and tissues, high dosage levels are administered. This is not usually economical and also raises toxicity issues. Such large quantities and the related toxicity problems have limited current cancer therapies [9, 10].

Y. Javed (✉) • K. Ali • Y. Jamil
Nano-Optoelectronics Research Laboratory, Department of Physics, University of Agriculture Faisalabad, Faisalabad 38040, Pakistan
e-mail: myasi60@hotmail.com; khuram_uaf@yahoo.com; yasirjamil@yahoo.com

S.K. Sharma (ed.), *Complex Magnetic Nanostructures*,
DOI 10.1007/978-3-319-52087-2_11

The use of heat as a healing source for a variety of diseases has been observed for around 3000 years ago in India. Hippocrates (540–480 BC) used hot sand in the summer to cure diseases. Hyperthermia comes from Greek words *hyper*, meaning "raise," and *therme*, meaning "heat." The first use of *hyperthermia* in connection with cancer treatment was by a Roman doctor, Cornelius Celsus Aulus, who observed high thermal sensitivity to early-stage cancer [11]. In the Middle Ages, hyperthermia was used with respect to several disease treatments such as malaria, and the first proper work on hyperthermia was published in 1886 [12]. Although the idea of using heat to treat cancer has been around for years, results had not evolved according to expectations initially. In 1975, the first international congress on hyperthermia oncology in Washington represented a major step toward hyperthermia research activities in the scientific community. In later years, different groups on hyperthermia had formed in the USA, Europe, and Japan.

In hyperthermia, body tissues are subjected to elevated temperatures by means of external (alternating field) and internal (nanoparticle) devices (Fig. 11.1). Electromagnetic radiation demonstrates active interactions with tissues, which allows for potential applications in thermal therapies. Owing to their limitations for treatment in deep seated tissues, alternating magnetic fields in a frequency range up to 10 MHz offer great potential for treatment in deep tissue areas. Human tissues are usually diamagnetic and show negligible magnetic effects. However, AC magnetic fields induce eddy currents in any conducting Medium. These eddy currents finally subject to losses [14–16]. Clinical studies have been performed to estimate the AC field tolerance level in the human body [17]. The results showed that the acceptable level is confined to the product of the frequency and field strength [18–20],

$$fH_{\mathrm{a}} < 4.85 \times 10^{8}\ \mathrm{A.m/s}. \tag{11.1}$$

It has been reported that cancer cells are more sensitive to temperature (approximately 42–48 °C) compared to normal cells (approximately 50 °C) and tumor development can stop in this temperature range [21, 22]. Temperature ranges for cancer treatment can be split into two parts; one is the hyperthermia range, in which temperatures between 41 to 48 °C are used for cancer treatment, while

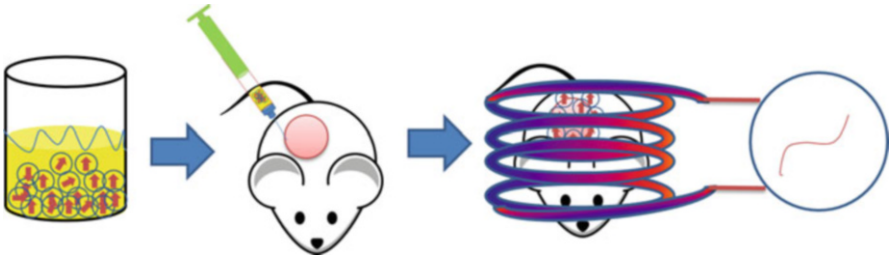

Fig. 11.1 Schematic of magnetic hyperthermia measurement (Reproduced with permission from [13])

the second is the thermoablation range, which uses temperatures above 47–56 °C [23, 24]. Thermoablation causes acute necrosis, coagulation, or carbonization of tissues, which is why it is not required in the majority of clinical hyperthermia treatments [25]. The efficient response of hyperthermia relies on the temperature rise and exposure time. For example, Valdagni and coworkers [26] compared responses in patients subject to 24% radiation therapy alone with the responses of those subject to 69% radiation therapy plus hyperthermia and noted an increase in local control of metastatic lymph nodes without a concomitant increase in toxicity. The researchers followed the two treatments (radiation therapy alone and radiation therapy plus hyperthermia) in random trials on metastatic lymph nodes in stage IV head and neck cancer patients for 5 years.

Hyperthermia treatments can be classified broadly into three groups: whole-body hyperthermia, regional hyperthermia, and local hyperthermia. Whole-body hyperthermia is usually used in cancer that can spread from its primary site (site of origin) to other organs; such cancer is called metastatic cancer [27]. The other two types of hyperthermia are more useful in localized tumors. These two types can be further subdivided into external, interstitial, and endocavity hyperthermia. Moreover, heat generation processes can also modify according to the target region and by other parameters controlling heat generation [28, 29].

For efficient hyperthermia, delivery mechanisms should be noninvasive, be highly tissue specific, and have the ability to produce high-intensity heat confined to a limited area in deep tissues [13]. The dose rate requires a balance between the quantity of magnetic fluid needed for therapeutic efficacy and damaging effects on normal cells [30]. Gilchrist and coworkers [31] were the first to report magnetic nanomaterials for hyperthermia in the 1950s and later years; magnetic nanoparticles had shown promising capabilities to satisfy all the aforementioned requirements [4, 32–37]. Magnetic nanoparticles have been used in diagnosing, imaging, and treating cancer with different techniques [38, 39]. Magnetic fluids can be delivered very efficiently to specific sites inside an organism noninvasively with the help of different drug delivery routes and subsequently heated using alternating magnetic fields at frequencies harmless to healthy tissues [40, 41]. Additionally, alternating magnetic fields can be used to direct magnetic nanoparticles to some extent for nonspecific remote localization [42]. Targeted localization can be attained by functionalizing nanoparticles with appropriate biopolymers. Magnetic nanoparticles have also shown a tendency to aggregate inside certain types of cancer tumors [43]. The majority of nanoparticles for hyperthermia consist of magnetite (Fe_3O_4) and ferrites with cobalt, nickel, and other substitutes. These materials range from nanometers to a few microns in size.

Currently, the focus has shifted toward single-domain nanoparticles, called superparamagnetic particles, owing to their high absorbance of power, at body acceptable magnetic fields and frequencies, as compare to multidomain nanoparticles, [13, 44, 45]. This type of magnetism arises in tiny ferromagnetic or ferrimagnetic nanoparticles where magnetic spins can flip randomly owing to temperature. In this case, when we measure the magnetization for much longer times than their relaxation time, the overall magnetization becomes zero, i.e., a so-called superparamagnetic

state. Nanoparticles can be magnetized by applying an external field that shows higher magnetic susceptibility than usual paramagnetic materials. The anisotropic energy of superparamagnetic nanoparticles corresponds to their volume. When the particle size decreases [46–49], the anisotropic energy also decreases, and at a certain threshold of particle size it can be equal to or less than the thermal energy k_BT. This implies that magnetization reversal can happen below this energy barrier. The overall magnetic moment can rotate freely, whereas internal moments stay magnetically intact, i.e., ferromagnetic or antiferromagnetic.

In summary, many research groups have investigated the ability of magnetic nanoparticles to generate heat in vivo using different types of nanoparticles, field parameters (different frequency and amplitude), and thermometry methods [47–49]. However, researchers continue to study the toxicity of nanoparticles [50], different cancer types [51–53], and field optimization and to improve biological targeting by more efficient drug delivery methods. This chapter covers the physical principles and different crucial aspects that can affect the heat efficiency of magnetic nanoparticles.

11.2 Physical Basis of Magnetic Hyperthermia

To understand the physics behind the generation of heat from nanoparticles under an AC magnetic field, a key point is to fine tune the properties of the nanoparticles for efficient hyperthermia treatment. Magnetic nanoparticles show heating effects due to heating losses during their magnetization reversal processes [4, 25, 54]. Although a magnetic field can be established by different methods, inductive coils are an efficient source owing to the uniform magnetic field inside the coils. The intensity of the field can be calculated by

$$H_a = \frac{NI}{L}, \tag{11.2}$$

where N is the number of turns of coils, I is the coil current, and L is the length of the coil. There are three main mechanisms responsible for these losses. First are eddy currents, which arise owing to friction heating; this mechanism is mostly developed in bulk materials (around 1 cm in size) [55]. Second is magnetic heating from hysteresis losses, which occurs in multidomain nanoparticles (at least 100 nm). Third and more relevant to nanoparticles is magnetic heating from relaxation mechanisms, i.e., Néel and Brownian relaxation mechanisms [in the nanometric range, i.e., 20 nm (for iron oxide), also called superparamagnetic nanoparticles] [56]. These mechanisms are discussed in detail in what follows.

11.2.1 Eddy Currents and Hysteresis Losses

The two less effective heat mechanisms are eddy currents and hysteresis losses that were initially considered for hyperthermia heat generation. When a changing magnetic field is applied on a conducting material, a swirling current is produced called an eddy current. By Lenz's law, the current moves so as to produce a magnetic field opposing the change, and for this, in a conductor, electrons move in a plane perpendicular to the applied magnetic field. This opposing tendency of the eddy current causes energy loss. In other words, it transforms the useful form of energy, i.e., kinetic energy, to heat. This heat formation is the main source of hyperthermia treatment in large particles. Eddy current escalates radially, therefore it is expected that maximum losses will be induced in sections with the highest cross-sectional area. If we consider a uniform magnetic field and cross-sectional area as a cylinder (Fig. 11.2a), the power generation can be calculated by integrating the time-averaged current density over the cross-sectional area:

$$P = \sigma(\pi \mu_0 f H_a)^2 r^2, \tag{11.3}$$

where σ is the bulk tissue conductivity, μ_o is the permeability of free space, f is the applied frequency, H_a is the applied field strength, and r is the effective radius.

This equation shows that current losses depend on the square of three factors, frequency, field strength, and radius. Therefore, losses will rise as we increase the frequency or applied field and be higher at the periphery of large cross-sectional tissues.

But eddy currents are not generated entirely from magnetic materials; tissues also have the capability to induce eddy currents owing to their low specific electrical conductivity, but their heating effect is far below the required therapeutic dose [57, 59]. Because eddy currents are induced mostly by bigger particles (a few millimeters in size), their contribution to heat generation is negligible when their size is reduced to the nanometer range.

11.2.2 Hysteresis Losses

As mentioned earlier, hysteresis losses are mainly due to multidomain nanoparticles. Ferromagnetic materials contain different regions in which there is uniform magnetization or all the magnetic spins align in one direction. These regions are called magnetic domains and each domain is separated by domain walls (Fig. 11.2). Domains emerged to reduce the overall magnetostatic energy of materials. When we apply an AC magnetic field to such materials, their magnetization aligns during the positive half cycle along the field and they demagnetize during the negative half cycle. This sequence of magnetization and demagnetization is usually represented in the form of a nonlinear curve called a hysteresis loop. The area

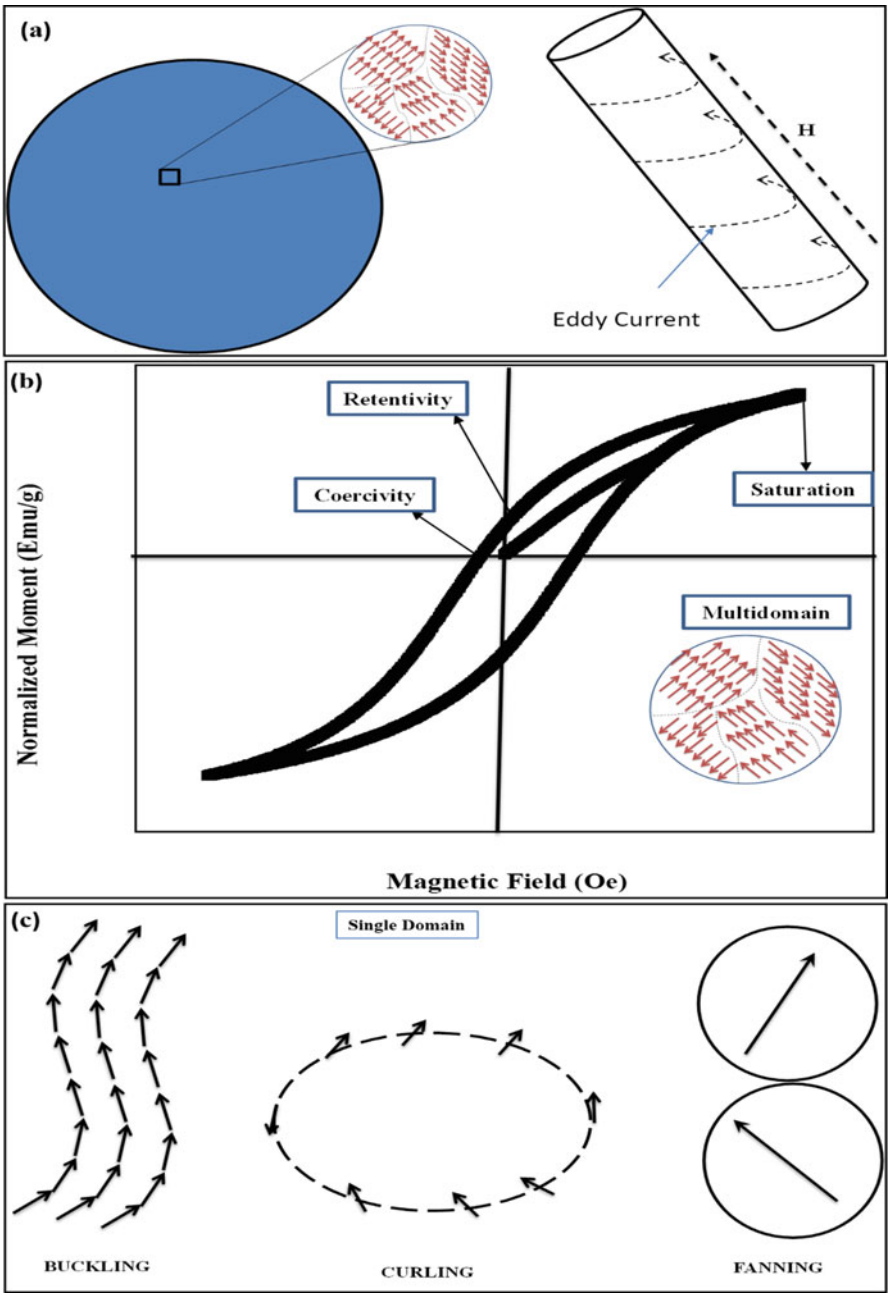

Fig. 11.2 (**a**) Schematic of eddy current. (**b**) Hysteresis of cobalt ferrite nanoparticles injected in mice at 10 K temperature using vibrating sample magnetometer. (**c**) Reversal mechanisms in single-domain ferromagnetic nanoparticles, buckling, curling, fanning. (Reproduced with permission from [57, 58])

under the curve represents both the strength of the magnetic material, i.e., hard magnetic material or soft magnetic materials, and heat loss during the AC cycle [60]. Actually, by the application of an external field, magnetic moments tend to minimize their potential energy by aligning in the direction of the applied field. In multidomain nanomaterials, these domains align and expand at the expense of neighboring domains. This movement of domain walls do not come back to their normal positions, when the field returns to zero and this behavior evolves hysteresis loop [61]. A hysteresis loop of cobalt ferrite nanoparticles injected into mice intravenously at 10 K is shown in Fig. 11.2b. Different points are described in the figure, such as saturation point, retentivity, and the coercive field. In nanomedicines, frequencies in the kilohertz to megahertz range and a field strength between $H = 0$–40 kA/m are commonly used [62].

The lack of retraceability of magnetization curves can also be observed in the absence of domain walls, i.e., in a single domain, where much lower values of coercivity than anticipated by the Stoner–Wohlfarth model were observed. The reversal processes here are very complicated, such as buckling, curling, and fanning. These processes are difficult to explain using classical physical models such as the Stoner–Wohlfarth model, in which uniform magnetization reversal in single-domain particles is observed. In contrast, Hergt and coworkers [63] found a power law for the field dependence of losses for a small-amplitude range. They formulated an expression that anticipated losses on the basis of the applied field parameters and particle size distribution [64]. Their experimental values and theoretical estimations provide specific loss power in the range of superparamagnetic nanoparticles. A schematic of three reversal mechanisms in the case of a single domain is shown in Fig. 11.2c [60].

11.2.3 Néel and Brownian Relaxations

At much smaller dimensions, i.e., a few tens of nanometers, a group of distinctive moments inside a magnetic particle is considered as a single giant spin that represents the total magnetization of the particle. At this size threshold, thermal fluctuations cause the flipping of the magnetization away from its normal state by controlling the magnetic energy. This phenomenon arises when the anisotropic energy barrier scales down to a particular position where thermal motion dominates this barrier. This thermally triggered process is called superparamagnetic [65]. The critical diameter for superparamagnetic behavior can be obtained by considering the spherical shape of a nanoparticle and modifying the relation used to illustrate the probability of relaxation. In the superparamagnetic phenomenon, although remanence and hysteresis mechanisms disappear, appreciable losses can still be observed owing to moment relaxation processes [66, 67].

Two relaxation mechanisms are involved in superparamagnetic nanoparticles: Néel relaxation and Brownian relaxation (Fig. 11.3). Néel relaxation involves the movement of all the spins in the particles and, hence, the magnetization direction,

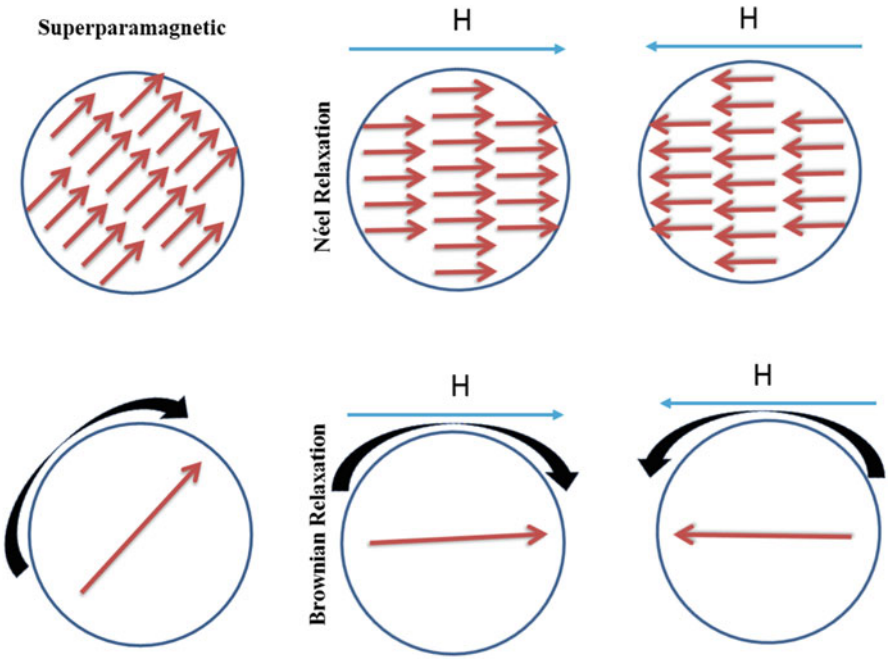

Fig. 11.3 Schematic of Néel and Brownian relaxation mechanisms of heat generation (Reproduced with permission from [4])

but not essentially the physical movement of the particle. These oscillations in the magnetization can occur in a specific time, called the relaxation time. These fluctuations develop above a certain critical temperature T_B. Below T_B, spin blocks are assumed to be fixed. Consequently, T_B is called the blocking temperature and suggests the superparamagnetic limit for steady magnetization. The time period of fluctuations can alter by changing the temperature and volume of a particle. Louis Néel [68, 69] proposed this temperature dependency and gave the following equation:

$$\tau_N = \frac{\sqrt{\pi}}{2}\tau_0 \frac{e^{\Gamma}}{\sqrt{\Gamma}}, \tag{11.4}$$

where

$$\Gamma = \frac{K_\mu V_M}{k_B T}. \tag{11.5}$$

Here, τ_o is the attempt time and $\tau_0 = 10^{-9}$ s, Γ is the ratio of anisotropy to thermal energies, K_μ is the anisotropy energy density, V_M is the volume of the suspension, and k_B is Boltzmann's constant.

Néel relaxation gives the vital relationship between anisotropic energy K and thermal energy kT, which provides the relaxation of the inner magnetic core. Brownian relaxation depends on the viscosity of the fluid and hydrodynamic volume of the nanoparticle [70]. In this relaxation, the particle itself can rotate and align with the external field. This movement depends on the hydrodynamic constraints of nanoparticles and suspended medium. It is also governed by the characteristic time. This characteristic relaxation time can be determined by the rotational mobility of the suspended magnetic nanoparticles and is given by

$$\tau_{\mathrm{B}} = \frac{3\eta V_{\mathrm{H}}}{k_{\mathrm{B}} T}, \tag{11.6}$$

where V_{H} is the hydrodynamic volume, and η is the viscosity of the liquid solvent.

Néel relaxation emerges for smaller particle sizes as a dominant process, whereas above a certain size range, the Brownian relaxation mechanism is more prominent. For close to the critical size limit, both mechanisms can be observed and the total effect can be calculated by taking their geometric mean [71, 72]:

$$\tau = \frac{\tau_{\mathrm{B}} \tau_{\mathrm{N}}}{\tau_{\mathrm{B}} + \tau_{\mathrm{N}}}. \tag{11.7}$$

However, distinguishing the contribution of the two mechanisms is very challenging, and experimental studies have been performed to meet this challenge. Fortin et al. [54] found that cobalt ferrite and maghemite nanoparticles have lower specific absorption rate (SAR) values in intracellular endosomes than when dispersed in water. They observed that Brownian mechanisms were prominent in the case of cobalt ferrite and Néel relaxation for maghemite nanoparticles. Similarly, Zhang and coworkers used magnetite nanoparticles dispersed in polydimethylsiloxane (PMDS) and water to differentiate the two relaxation mechanisms. They concluded that there was higher specific absorption when magnetite nanoparticles were dispersed in water due to both mechanisms. However, an additional contribution arises due to Néel relaxation by increasing the frequency and strength of an alternating magnetic field [73].

11.2.3.1 Calculation of Specific Absorption Rate for Magnetic Hyperthermia

The basic relation between the magnetic field and applied electromagnetic field is

$$B = \mu_0 \left(H_{\mathrm{a}} + M \right). \tag{11.8}$$

The increase in the internal energy for a complete cycle can be determined by integrating the following relation:

$$U = -\mu_0 \oint M \, dH. \tag{11.9}$$

This relation shows that eddy currents and resonance factors can be neglected. Because both the applied field and magnetization are time dependent and the field is sinusoidal, both the applied field and magnetization can be written in terms of field strength and frequency:

$$H(t) = H_{\mathrm{a}} \cos(2\pi ft), \tag{11.10}$$

$$M(t) = H_{\mathrm{a}}\left(\chi' \cos(2\pi ft) + \chi'' \sin(2\pi ft), \right. \tag{11.11}$$

where χ' and χ'' represent the in-phase and out-of-phase components of magnetic susceptibility, respectively. By solving and simplifying these equations, a final relation for the SAR is obtained:

$$\mathrm{SAR} = \mu_0 \pi \chi_0 f H_0^2 \frac{2\pi ft}{1 + (2\pi ft)^2} \sim \left[\frac{w}{m^3}\right]. \tag{11.12}$$

The heat generation of magnetic nanoparticles is generally presented in units of W/g. The heat produced per unit volume can be calculated by the product of the SAR value and the concentration of nanoparticles [58]. When the heat reaches a specific area of infected tissues, the temperature above the therapeutic threshold of 42 °C can be managed for half an hour to kill cancer cells. Nanoparticle size has a significant influence on relaxation mechanisms and maximum heat observed at a particular radius according to the type of magnetic material. Figure 11.4 shows the size-dependent heating curves for Fe_3O_4 and γ-Fe_2O_3. The SAR peak position depends mainly on the anisotropy of the materials; however, the frequency, viscosity, and temperature also have a slight effect [58]. Maghemite nanoparticles have high SAR values at sizes around 11–12 nm. The size dependency suggests that polydispersity ultimately will be an important factor. A narrow size distribution will be more useful for hyperthermia than highly polydisperse fluids. Motoyama et al. [74] studied the SAR generation of magnetite nanoparticles of 13 different sizes under different alternating magnetic field conditions. They considered the nanoparticles according to their surface area. The particle size ranged from 10 to 120 nm. They observed that the two highest values of SAR between 12 and 190 W/g, for different frequencies and values increased by increasing the intensity of the field. Particles with a smaller specific area had a strong influence on the intensity of the field compared to larger particles.

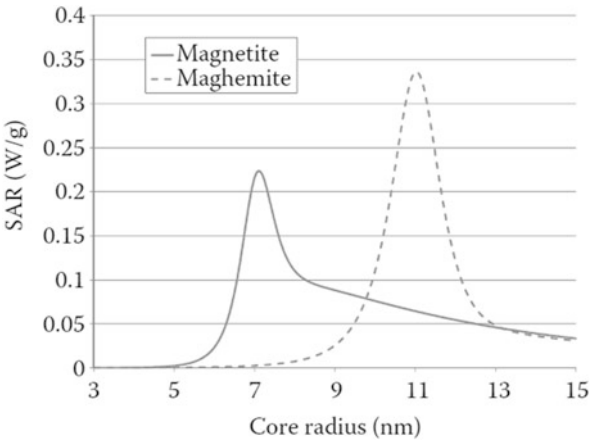

Fig. 11.4 Comparison of size-dependent SAR values for iron oxide (magnetite and maghemite) in water. Field strength, 10 kA/m; frequency 250 kHz [58] (Reproduced with permission from [58])

11.3 Magnetic Fluids for Hyperthermia

Owing to the notable heat loss in an AC magnetic field, a number of heat mediators have been established. Mediators are nanomaterials that have the ability to produce high heating power per particle in unit mass. Therefore, various types and shapes of magnetic nanoparticles have been investigated and used as a source of heat generation. These materials include metals such as Fe, Mn, Co, Ni, Zn, Gd, Mg, and their oxides; in particular, iron oxide–based nanomaterials have been explored extensively for their potential in hyperthermia [60, 75–78]. Superparamagnetic iron oxide nanoparticles have shown excellent properties for heat mediation. In addition, different ferrites, for example, $CoFe_2O_4$, $Li_{0.5}Fe_{2.5}O_4$, $NiFe_2O_4$, $ZnFe_2O_4$, $CuFe_2O_4$, and $MgFe_2O_4$, have also been considered for hyperthermia [79–84]. Zinc-rich ferrite nanoparticles 11 nm in size are capable of self-regulated magnetic heating in local glioma therapy [85]. Ferromagnetic composite nanoparticles, such as iron-doped gold [86], zinc manganese–doped iron oxides ($Zn_xMn_{1-x}Fe_3O_4$) [87], and zinc manganese gadolinium–doped iron oxides [87], have also been investigated as potential candidates for hyperthermia. However, iron oxide nanoparticles are the main priority of researchers owing to their lower toxicity, biocompatibility, and metabolization in the body [88]. Although the aforementioned nanomaterials show an overwhelming response to external AC magnetic fields, their stability under different conditions is also very critical.

11.3.1 Solvent Media

SAR values depend on the viscosity of the medium in which the nanoparticles are suspended. Heirgeist et al. [89] probed the heat generation capability of ferrofluids in molten and solidified gel. There was a considerable power loss in the liquid

phase compared to the solid phase. A more detailed study was performed by Fortin and coworkers [54] to distinguish the contribution from Brownian and Néel relaxation mechanisms. It was observed that with a more viscous medium (glycerol is 500 times more viscous than water), the contribution from Brownian relaxation fizzled out and the main contribution came from Néel relaxation, though Brownian mechanisms were prominent in the case of water for particle sizes above 9 nm (cobalt ferrite) and 17 nm (maghemite). The Néel contribution was frequency dependent. At a frequency of 1 MHz, the Néel contribution was highest for particle sizes of 7 nm (cobalt ferrite) and 14 nm (maghemite). However, there is still a need to explore the influence of viscosity on SAR values.

11.3.2 Anisotropy of Nanoparticles

Another important factor is growing nanoparticles with high anisotropy (controlled shape or monocrystalline). Nanoparticles have been studied in different size distributions as well as in different shapes (spherical [90], cubes [91], flowers [92]). Regular-shaped iron oxide (magnetite or maghemite), i.e., nanocubes, exhibit remarkably improved efficiency over their spherical counterparts [93]. Even iron oxide nanoflowers (20–25 nm) have better SLP values. Nanoflowers are actually multicore nanoparticles oriented in such a way as to produce a monocrystalline structure. This internal collective organization modifies their magnetic properties, which enhances their heating efficiency significantly [92] (Fig. 11.5).

11.3.3 Biological Environment

Usually hyperthermia studies are performed in biological environments (model medium, cell culture, or mice) that nanomaterials encounter when they go in vivo [95]. The high surface-to-volume ratio of nanoparticles increases the possibility of undergoing chemical and physical transformations owing to this biological microenvironment, which can affect the technologically relevant properties of nanomaterials [96, 97]. These transformations can lead to crystal dissolution and generate different ions. Such ions can be very toxic because they can induce hydroxyl radicals by a Fenton reaction that can damage DNA, proteins, and lipids in vivo [98, 99]. Different factors can modulate these transformations such as the functionalization of nanomaterials (organic/inorganic) and the nature of the material [100].

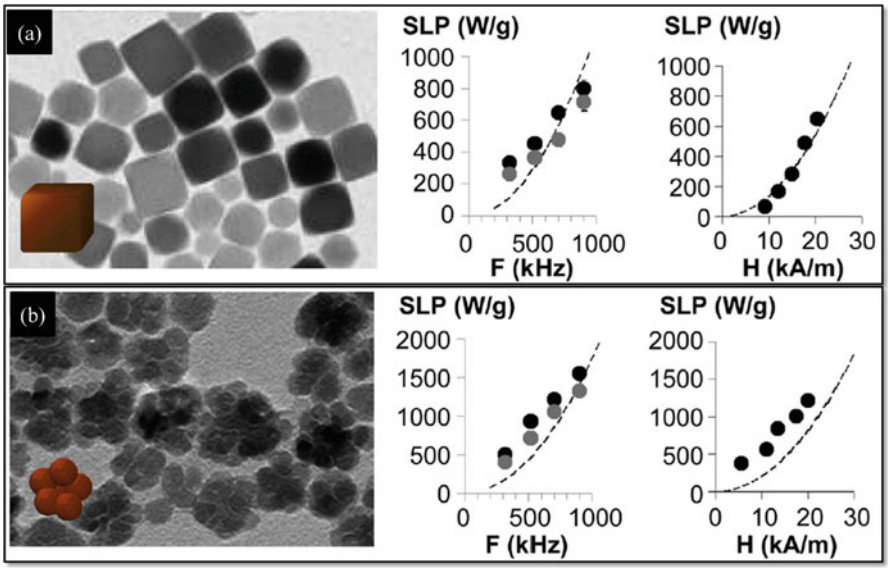

Fig. 11.5 TEM micrograph (*left*) and heating generation abilities [*right*, SLP (w/g) as a function of frequency and strength of applied magnetic field], iron oxide nanocubes with side face of approximately 18 nm. (**a**) Iron oxide nanoflowers approximately 25 nm in size. (**b**) SLPs were measured by making the fluids in water (*black circles*) and in glycerol (*gray circles*). The dotted lines indicate the poor agreement with linear response theory [94] (Reproduced with permission from [94])

11.3.4 Synthesis Protocols

The properties of nanomaterials largely depend on the synthesis protocols because magnetic properties can change with morphology and structure [101]. There is still a need to develop good synthesis methods to produce nanoparticles that have controlled sizes and shapes, have narrow distributions, and are free of crystal defects. The two major issues in the chemical methods are the formation of monodisperse nanostructures and the reproducibility of reactions. For controlled synthesis, nucleation should be separated from growth, and there should be no nucleation during the growth process [102]. By considering these conditions, various physical, chemical, and biological methods have evolved during the different research stages. Physical methods are mostly used in engineering and electronics, whereas chemical and biological protocols are used to produce nanomaterials for biomedical applications. These methods include coprecipitation [103], thermal decomposition [104], microemulsion [105], hydrothermal synthesis [106], polyols [107], sol-gels, combustion, and others. Each method has its own advantages and disadvantages that make it suitable for the synthesis of certain nanomaterials. Every protocol has a certain working solvent. For hyperthermia, we need nanoparticles' suspension in water, so the nanoparticles go through a ligand exchange process before they are made water dispersible [108].

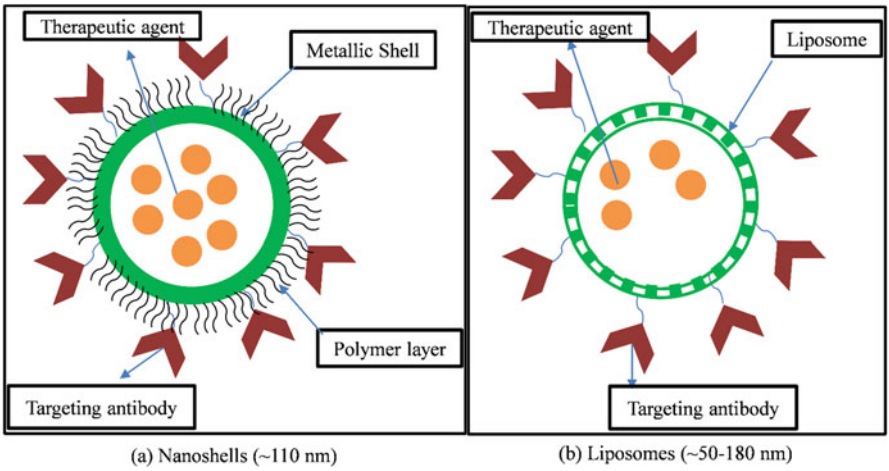

Fig. 11.6 Example of multifunctional nanocarriers for cancer treatment. A metal can be used to encapsulate the therapeutic nanoparticles followed by functionalization of biocompatible polymer and targeted biological antibodies. (**a**) Liposomes can also be used as carrier vehicles since they contain at least one lipid bilayer. (**b**) Reproduced with permission from [110]. Copyright (2009) American Chemical Society

11.3.5 Multifunctionality

The coupling of nanoparticles with other functional species (organic or inorganic materials) can further enhance their efficiency for heating [109]. Multifunctionality provides targeting, imaging, sensing, and therapeutic payloads simultaneously (Fig. 11.6) [110]. These multifunctional nanoparticles have significantly improved the diagnosis and treatment of prostate cancer [111]. Multifunctional nanoparticles for specific targeting as well as for optical tracking using a two-photon fluorescent probe have also been formulated. This type of nanoparticle has been adopted for the magneto-cytolysis of MCF-7 and UCI cancer cells by applying a DC magnetic field with additional optical tracking properties [112].

11.4 Biocompatibility

To develop nanomaterials for in vivo applications, nanoparticles must be acceptable to the body, in other words, nanoparticles should be biocompatible [39]. Because these nanomaterials are not a part of our body, bare nanoparticles can be rejected by macrophages very rapidly from the bloodstream prior to their use for a given application [113]. For example, dextran-coated Fe_3O_4 nanoparticles after IV administration in rats cleared very rapidly (half-life of 10 min) initially, then slowed down after some time (half-life of 92 min). During the initial 2 h, particles

spread throughout the whole body, including the liver and spleen. However, over time, the particles accumulated in the macrophages of the splenic marginal zone. The particles piled up in this region for 48 h, after which there was a decrease till day 25. Iron oxide stores in Kupffer cells of the liver result in slow accumulations, [114]. Iron oxide even persists for a long time in the body, we observed iron oxide–gold dimers in mice even after 1 year of their administration, which confirms their long stay in the body. Figure 11.7a–e shows the iron oxide–gold dimers present after 1 year in the spleen. The nanoparticles were injected intravenously. Although the iron oxide part of the dimers had been degraded, we observed gold particles as large aggregates, small chains, and separate particles (Fig. 11.7b) [115]. In the case of hyperthermia, an AC magnetic field cycle needs to be applied after some specified amount of time, and nanoparticles should stay inside the body at the target site for a longer period of time [45]. All these concerns demand biocompatible nanoparticles. It is usually believed that nanoparticles are eliminated from the body following therapy, which is not necessarily the case. Therefore, the toxicity of nanoparticles and the functionalization of materials are major concerns for developing nanoparticles as heating sources for hyperthermia [116]. In addition, it can use to prevent opsonization and the formation of protein corona on nanoparticle surfaces, when introduced into blood compartments. Therefore, nanoparticles should be characterized for their physicochemical and physiological properties to ensure a longer circulation time [117].

Nanoparticles are made biocompatible by their surface modifications, usually by applying a coat of biocompatible molecule, such as dextran, glucose, polyvinyl alcohol (PVA), or phospholipids [118]. This coating layer provides a channel between the nanoparticle and the target site on cells and it provides colloidal stability. The colloidal stability depends on the particle size, charge, and surface chemistry in order to avoid gravitational forces and steric and coulomb repulsions [119]. There are specific binding sites on the surface of cells that are usually targeted using antibodies such as folic acid. Antibodies have the tendency to bind to their corresponding antigens, which results in highly accurate cell labeling. The attachment of folic acid can increase the cytotoxicity against folate receptors, but it had a mild effect on A549 cells [120, 121]. Nanoparticles are usually coated by organic polymer layers, and inorganic coatings, such as silica and gold, have also been developed [122]. These inorganic coatings protect nanoparticles from the environment and provide additional properties of the coating material such as the plasmonic properties of gold. The thin gold layer it heated up itself under an alternating magnetic field during hyperthermia process [123]. In fact, gold-coated iron oxide produces more heat compared to iron oxide alone [124]. Javed et al. [125] investigated the influence of gold layers with different nominal thickness (3, 5, and 7 nm) on the degradation mechanisms of iron oxide nanoparticles (Fig. 11.8a–c). A layer 3 nm thick that forms 3D clusters of gold on nanoparticles was not as efficient as a later 7 nm thick to control degradation. A continuous layer forms with a nominal thickness of 7 nm and serves as an effective shield against surface corrosion. The loss of the iron contents of single nanoparticles was followed by the use of single-particle EDX analysis in scanning transmission electron microscopy (STEM) mode.

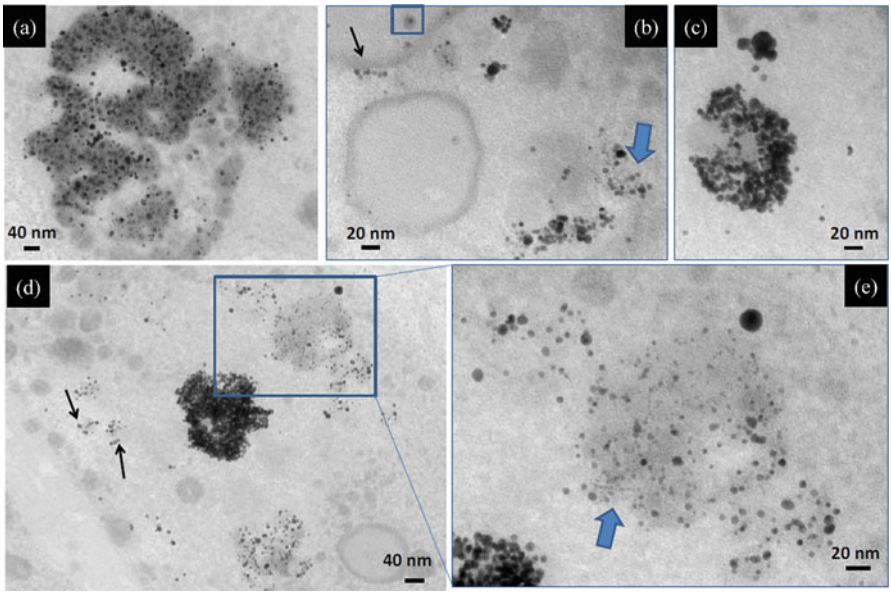

Fig. 11.7 (**a–e**) Amphiphlic polymer–coated iron oxide–gold dimers in spleen after 1 year following intravenous (IV) administration. Isolated heterostructures can still be observed (*blue box*) (**b**), but the majority are a gold moiety of the heterostructure assembled as large aggregates (**c**), or gold chains (*black arrows*); (**d**) degraded gold entities can also be observed in (**e**) [115] (Reproduced with permission from [115]. Copyright (2015) American Chemical Society)

There was a rapid loss of iron with respect to gold in a layer of gold with a nominal thickness of 3 nm, whereas there was almost no loss in the case of the 7 nm gold layer (Fig. 11.8d).

Physicochemical properties of nanoparticles, such as their size, shape, composition, charge, and surface chemistry, can play a significant role in the pharmacokinetics of nanoparticles [126]. These factors administer the flow of nanoparticles in different parts of an organism and also control circulation time, nanoparticle intracellular trafficking, drug release, and toxicity [127]. Nanoparticles less than 100 nm in size have a longer circulation time. But the size of nanoparticles can also influence the surface pressure and adhesion forces [128]. Nanoparticles have extraordinary interfacial chemical and physical reactivity owing to a high surface area. Generally, kidneys can eliminate nanoparticles less than 6 nm in size more rapidly compared to larger ones functionalized by, for example, polymers and lipids [129]. Larger particles are usually stored in the spleen and liver and more specifically in the lysosomes of macrophages cells, where they are processed by the acidic environment, different enzymes, and proteins [116]. The factors related to biocompatibility are discussed briefly in this section.

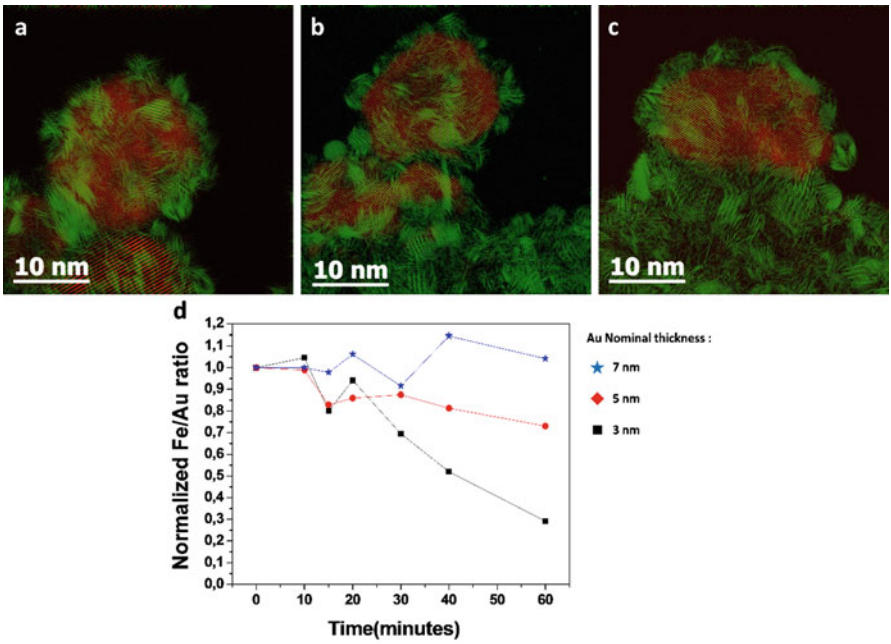

Fig. 11.8 Low-pass-filtered, high-resolution images of nanoparticles covered by layers of gold with nominal thicknesses of (**a**) 3 nm, (**b**) 5 nm, and (**c**) 7 nm. (**d**) Follow up of iron loss by chemical composition analysis in STEM mode [125] (Reproduced with permission from [125])

11.4.1 Opsonization

Interactions of nanoparticles with bound ligands and cellular receptors are governed by the morphology of the nanoparticles and the density of the polymer on the surface. The functionalization of nanoparticles helps to keep them for a longer time in the body and limits their nonspecific distribution [130]. Intravenous administration has a drawback in the form of rapid clearance of nanoparticles from the bloodstream as a result of the opsonization process. This is the process of attaching any blood serum component, which can help to identify phagocytes. Macrophages such as Kupffer cells and others in the liver cannot precisely recognize nanoparticles themselves but instead use opsonized proteins attached to the surface of the nanoparticles. The most common opsonized proteins are C3, C4, C5, and immunoglobuline. The binding and clearance of nanoparticles by nonphagocytic cells can also be influenced by the adsorption of blood plasma proteins. For instance, after binding of proteins such as C3b, C4b, or iC3b, nanoparticles can then interact with platelets and erythrocytes [131].

To overcome this problem, nanoparticles are usually coated with a variety of polymer materials that can produce a hydrophilic steric barrier [132]. This manipulated steric boundary should oppose surface adsorption processes and as

a result reduce the chances of nanoparticles' clearance by macrophages in the blood stream. This also increases the possibility of nanoparticles' targeting specific nonmacrophage elements. The pharmacokinetics of these modified nanoparticles depends on the density of the polymer materials [118]. Al-Hanbali et al. [133] showed that the attachment of at least 11,500 poloxamine molecules was required on the surface of 230 nm polystyrene nanoparticles to overcome opsonization and increase the circulation time compared to bare nanoparticles. Under these circumstances, a layer of polyethylene oxide with the appropriate density can form on the surface of nanoparticles. It was assumed that polymeric chains have a brushlike configuration to reduce prompt complement activation and increase circulation time. A thin polymer layer or low surface density can speed complement activation and, as a result, shorten circulation time. Thus, a higher polymer density on the surface of nanoparticles allows for steric stabilization, limits protein absorption, and increases circulation time.

11.4.2 Surface Charge

The surface charge of nanoparticles also plays a crucial role in subsequent intracellular processing events. Therefore, the realization of interactions between cells and nanoparticles is key to determining the uptake and localization of nanoparticles [134]. There is faster uptake in vivo when nanoparticles have a positive surface charge versus a neutral or negative charge owing to the negative charge on the surface of cell membranes. This is done by the electrostatic attractions between two surfaces. However, positively charged particles clear more quickly from the blood and cause hemolysis and platelet aggregation. Thus a smaller size, neutral or negative zeta potential, and PEG coating of the particle surface are highly influential factors for increased circulation time in the blood after IV administration [135].

11.4.3 Protein Corona

Another important factor is the coating of a protein layer on the nanoparticle in biological matrices, the so-called protein corona. There are 1000 different proteins with different concentrations present in the blood plasma. Consequently, upon injection of nanoparticles into the body, different biological entities try to adsorb onto nanoparticles' surface [136]. However, proteins present in higher concentrations adsorb first, followed by the replacement of high-affinity proteins. They can transform and protect the surface of xenobiotic particles and control their biological properties and, consequently, their behavior in the micro environment. Physicochemical properties, type of physiological environment, and exposure time are critical factors governing the structure and composition of corona formation [137]. The protein corona confers a new biological identity to nanoparticles, which

controls physiological responses such as aggregation, cellular uptake, circulation time, kinetics, transportation, accumulation, and toxicity [138].

The formation of a protein corona depends on the binding affinities between proteins and nanoparticles and protein–protein interactions. Proteins with high affinity are bound more tightly, and a corona so formed is called a hard corona. These proteins cannot desorb easily from the surface of nanoparticles. Proteins that adsorb with low affinity form a soft corona. These are loosely bound proteins. The concern raised by the adsorption of proteins or protein corona formation has been explored very little because it is a very complex situation when nanoparticles are administered directly into a living organism. Additionally, there is no general protein corona for all nanomaterials; in fact, protein corona formation is distinct for the different nanomaterials and there are many dependent factors [139].

11.4.4 Toxicity

The toxicity of nanoparticles and functionalized polymers is usually determined by many factors, such as dose rate, composition, administration method, biodegradability, surface chemistry, shape, and many more. An understanding of animals' and nanomaterials' toxicity profiles is necessary to guarantee their safe use [140]. It is usually believed that nanoparticles are more toxic than larger particles of the same chemical composition and that toxicity is inversely proportional to particle size [141]. Surface modification of nanoparticles is a vital tool in reducing toxicological effects. In addition, during oral or dermal exposure or inhalation, nanoparticles can accumulate in the lungs and may absorb across the gastrointestinal tract. A common method of evaluating in vitro toxicity is by the use of fluorescent dyes to determine cell death by necrosis and apoptosis. Cell death because of injury is called necrosis and is usually identified by membrane breakage and discharging to other cell surroundings, which results in an immune response, whereas apoptosis is systematic cell death where cells retain their membrane intact till the last stage, apoptosis. Then the cell constituents transform into amino acids and nucleotides that can be recycled and used again by nearby cells. Superparamagnetic iron oxide nanoparticles can activate apoptosis itself in cells; consequently, necrosis cannot be used to measure this action in the early stages in vitro and can only be useful in the late stages when the cell membrane disintegrates [142]. Therefore, it is necessary to measure both necrosis and apoptosis simultaneously. More specifically regarding the toxicity of iron oxide nanoparticles in vivo, after infiltrating into cells, these nanoparticles reside in endosomes/lysosomes and then, after processing, are released into the cytoplasm and sequestered in ferritin proteins. It has been observed that after inhalation, they accumulate largely in the liver and spleen and in small quantities in the lungs and brain. Their toxic effects appear in the form of cell lysis, inflammation, and a reduction in cell viability. Naqvi and coworkers [143] observed that a low dose (20–200 μg/mL, exposure time 2 h) of iron oxide (30 nm) caused more cell toxicity than a high dose (300–500 μg/mL, exposure time 6 h).

However, there was 20% less cell death when dextran-functionalized iron oxide nanoparticles (100–150 nm, 1 mg/mL) were incubated for 7 days in human macrophages. It is commonly believed that cell death is caused by the generation of reactive oxygen species as a result of Fenton reactions. These produce oxide and hydroxyl ions that can stimulate DNA damage and the oxidative degradation of lipids by extracting electrons.

In brief, for hyperthermia, nanoparticles should be water dispersible, biocompatible, smaller in size, negatively or neutrally charged, and nontoxic. However, there are still a few limitations on the efficient delivery of nanoparticles at target sites. An embolus can form in the blood vessels owing to the aggregation of nanocarriers. Second, complications can arise as a result of the focus on nanoparticles from animal models because of the larger gap that exists between intended sites and magnets in such models.

11.5 Measurement Systems

Although much work has been done on magnetic hyperthermia based on parameter control (e.g., size, shape, distribution) to improve the heating capabilities of nanoparticles, few sophisticated systems have been made available on the market for measuring specific loss power. Most systems designed for experiments are built by different research groups. They use these homemade systems to measure heat loss in the form of nanoparticle fluid and for experimentation in mice. On the other hand, some commercial devices are the magnetherm by nanoTherics (Newcastle under Lyme, UK), the DM100 series from nB nanoScale Biomagnetics (Zaragoza, Spain), EASYHEAT from Ambrell (Scottsville, NY, USA), or the MGF1000 in vitro magnetic field generator by the European Institute of Science AB (Lund, Sweden). These commercial devices have offered a range of variations in AC magnetic fields, i.e. frequency, amplitude, or flux density. These devices provide reliable and reproducible results for nanoparticle heating.

Regarding the homemade systems for hyperthermia that are being used by different research groups, these devices are usually based on simple resonant RLC circuits to create an AC magnetic field with a copper coil [54, 144–146]. Researchers all over the world are using locally made devices applying the aforementioned idea to make certain modifications, for example, changing the coil diameter, number of turns, or cooling agents. Here we will discuss a few systems that have been reported in the literature.

Fortin et al. [54] tried to distinguish the contributions of Néel and Brownian relaxation mechanisms with respect to specific loss of power. They used a device with a copper coil 16 mm in diameter having a frequency range of 300 kHz to 1.1 MHz and an amplitude up to 27 kA/m. Variations in frequency and amplitude are made using a variable capacitor (10 pF–4 nF) in series and self-inductance of 25 μH. To avoid heat generated by the coil, continuous circulation of nonane was maintained during measurements. A small sample volume of 300 μL was

used so that a homogenous magnetic field could be established on the particles A fluorooptic thermometer was used for temperature measurements. The researchers presented quantitative magnetic hyperthermia data matching with theoretical predictions considering relevant parameters such as size, materials, solvent, and field characteristics. Ma and coworkers [145] investigated the size dependence of iron oxide nanoparticles on heat generation. They used a three-loop copper coil with a frequency of 80 kHz and amplitude of 32.5 kA/m for calorimetric measurements. In addition, they used an asbestos sleeve to avoid excessive heat produced by the copper coil. An alcohol thermometer was used to measure the heat generated by the particles. Magnetic fluids were prepared in water at a concentration of 2 g/L. The maximum SAR value (75.6 W/[g of Fe]) was observed at a particle size of 46 nm. Further increases in the particle size showed a low heat generation efficiency. Sadat et al. [147] used a 10-turn coil that was 84 mm long and had an inner diameter of 39 mm. A sinusoidal 13.56 MHz frequency signal was generated by a radio frequency generator. Cold water circulation was used to cool down the coil from the high AC current. A fiber optic temperature sensor (FOT-L-SD) was connected to detect the temperature signal. The researchers observed high SAR values for uncoated nanoparticles compared to coated or confined nanoparticles in another material such as iron oxide in a Si shell. They attributed the high absorption rate in uncoated nanoparticles to Néel relaxation and hysteresis losses whereas dipole–dipole interactions caused lower SAR values. The schematics of the system are shown in Fig. 11.9a–c.

A safe and effective external magnetic field is required to stimulate implanted nanoparticles. Major issues for designing such a system are field uniformity, patient convenience, and proficiency at working on the entire body. Multiturn inductive coils, discussed earlier, satisfy the requirements for small animal preclinical trails [148].

Clinical trials: Although the European Union (EU) approved several iron oxide nanoparticles, the US Food and Drug Administration (FDA) has endorsed three nanoparticles (Feraheme, polyglucose coated superparamagnetic iron oxide nanoparticles, dextran-coated iron oxide (Feridex), and silicon-coated iron oxide (GastroMark). Feridex and GastroMark were later withdrawn over concerns regarding their long-term toxicity in vivo [149]. Nanoparticle-based induction hyperthermia (thermal ablation) was first investigated by Kida et al. [150] for brain tumor treatment in 1990. Fe-Pt alloy particles were studied in connection with metastatic brain tumor along with radiation therapy. The particles were of millimeter size (15–20 mm long with a diameter of 1.8 mm). The temperature of the tissues raised up to 46 °C during treatment. In two cases, there was complete destruction of tumor (complete response), whereas in one case, a 50% tumor volume reduction occurred (partial response). In another study, 23 patients with brain tumor were treated by the aforementioned method and the response rate was 34.8% on average [151]. However, there are few studies on intracranial tumor therapy, apparently because of complications such as that it required infiltration through

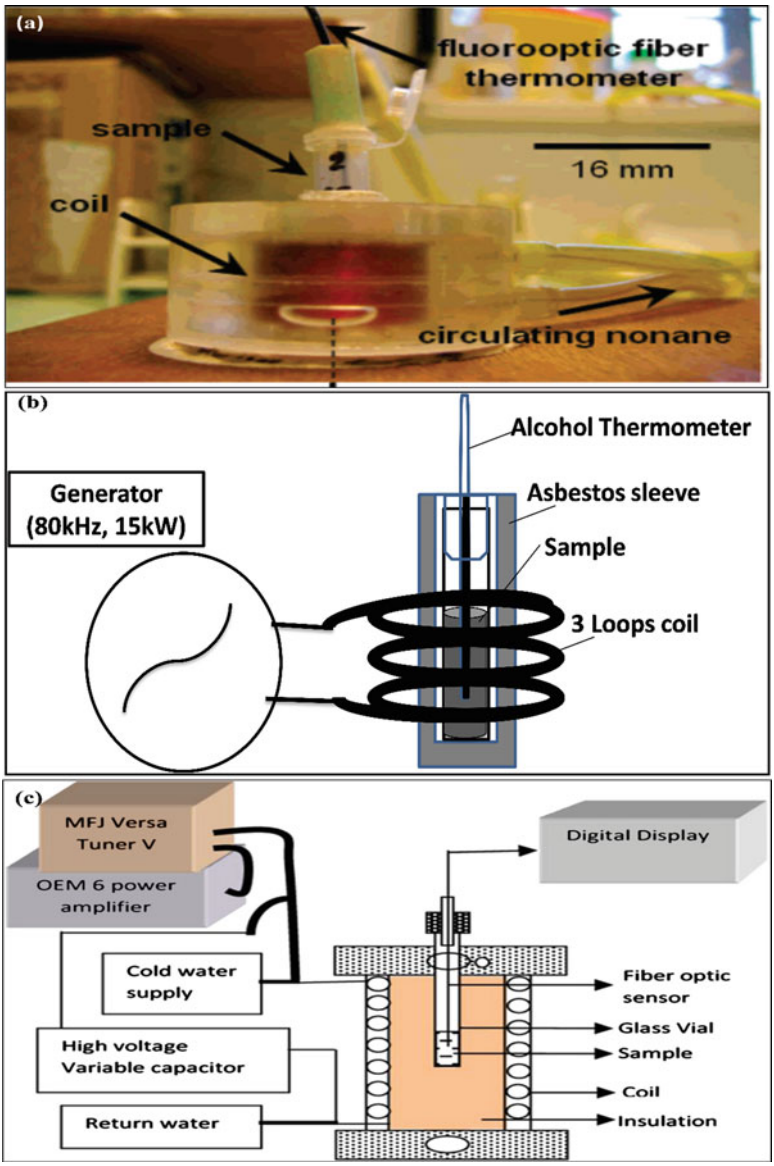

Fig. 11.9 Homemade systems used by different research groups: (**a**) [54]; (**b**) [145]; (**c**) [147] (Reproduced with permission from [54, 145, 147]. Copyright (2007)American Chemical Society)

the skull, which can cause significant trauma. Another implication is the access of nanoparticles to the tumor site by passing through healthy brain tissue, which can also be critical. These limitations hamper the application of induction hyperthermia in other brain tumor applications [152].

Hyperthermia based on superparamagnetic nanoparticles has also been applied in combination with other therapies. Aminosilane-coated iron oxide nanoparticles 12 nm in size were administered intratumorally following tumor resection. Treatment by radiotherapy and 100 kHz variable magnetic field combined was compared with traditional radiotherapy alone. Patient survival was prolonged from 13.4 months to 23.2 months and the tumor revival time was also enhanced [153, 154]. Patient rehabilitation was evaluated by MRI and CT overlay (Fig. 11.10a–f). Phase 1 trails showed no systematic toxicities upon intratumoral administration. However, patients felt some discomfort owing to the rise in temperature around the tumor to 44 °C [156]. Magnetic hyperthermia coupled with chemotherapy generated collective malignant cell death.

Methoterxate-functionalized iron oxide nanoparticles (10 nm) were activated by a 300 kHz, 130 Gs alternating magnetic field. The combined therapy produced greater apoptotic response [157]. A phase II study was performed in recurrent glioblastoma. The study revealed the utility of integrating magnetic nanoparticle–based hyperthermia immediately before or after radiotherapy.

11.6 Conclusions

The generation of localized heat by magnetic nanoparticles and an alternating magnetic field in the area surrounding malignant cells has the potential to kill cancer cells. The method can be employed alone or coupled with radio- or chemotherapy to enhance its efficacy. Despite all the advances, proper technology development remains immature. A few crucial enhancements must be made to improve the clinical viability of magnetic nanoparticle–based hyperthermia:

1. The functionalization of nanoparticles is required for biocompatibility, biological recognition, toxicity reduction, and nanoparticle life cycle regulation.
2. Although iron oxide nanoparticles show reasonably high SAR values, improvements can be made by higher magnetic moment nanoparticles. This includes iron–iron oxide composites, magnetosomes, and iron–cobalt core shell structures.
3. By incorporating magnetic nanoparticles into multifunctional systems, their therapeutic, imaging, and diagnostic capabilities can be improved.
4. An alternating magnetic field should selectively heat the nanoparticles, engulfing the tumors and avoiding the accumulation of nanoparticles in other regions, for example, the liver or kidney. In addition, alternating waves can deliver enhanced power input.
5. Nanoparticles should absorb sufficient power to reach cytolytic tumor temperatures but maintain the surrounding tissue temperature at manageable levels.

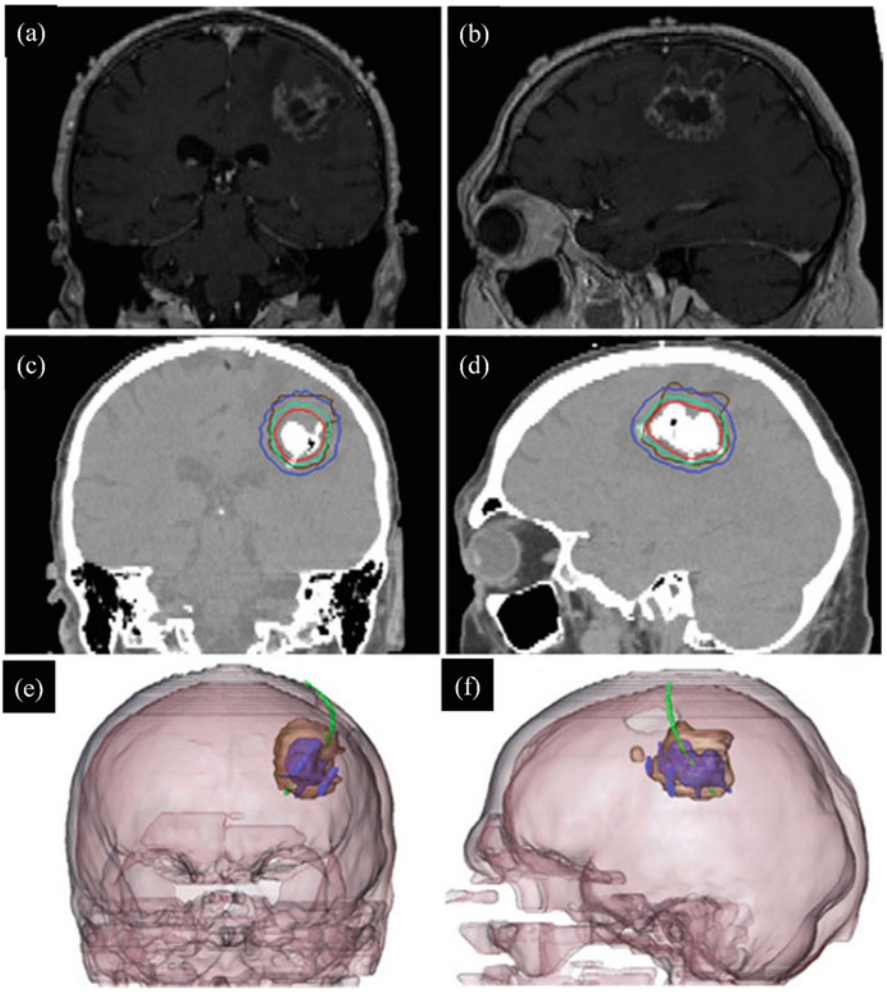

Fig. 11.10 Glioblastoma recurrence. (**a**, **b**) Control brain MRI. (**c**, **d**) Magnetic nanoparticle deposits in brains are shown in the form of hyperdense areas (CT image). Calculated treatment temperatures are represented in the form of isothermal lines, minimum 40 °C (*blue*), maximum 50 °C (*red*). The *brown line* shows the tumor area. (**e**, **f**) 3D reconstruction of merged MRI and CT [155] (Reproduced with permission from [155])

6. Noninvasive in vivo tracking of nanoparticles is necessary to confirm that nanoparticles reside at the target site.
7. The efficacy of the method should be accurately evaluated so that concerns related to dose rate, temperature, exposure time, administration procedure, and repetition of treatments can be addressed.

References

1. Caster JM, Patel AN, Zhang T, Wang A (2016) Investigational nanomedicines in 2016: a review of nanotherapeutics currently undergoing clinical trials. Wiley Interdisciplinary Reviews: Nanomedicine and Nanobiotechnology (In press)
2. Del Burgo LS, Hernãindez RM, Orive G, Pedraz JL (2014) Nanotherapeutic approaches for brain cancer management. Nanomedicine: Nanotechnology, Biology and Medicine 10: e905–e919
3. De Jong WH, Borm PJA (2008) Drug delivery and nanoparticles: applications and hazards. Int J Nanomedicine 3:133
4. Deatsch AE, Evans BA (2014) Heating efficiency in magnetic nanoparticle hyperthermia. J. Magn. Magn. Mater. 354:163–172
5. Deraco M, Kusamura S, Virzì S, Puccio F, Macrì A, Famulari C, Solazzo M, Bonomi S, Iusco DR, Baratti D (2011) Cytoreductive surgery and hyperthermic intraperitoneal chemotherapy as upfront therapy for advanced epithelial ovarian cancer: multi-institutional phase-II trial. Gynecol Oncol 122:215–220
6. Gobbo OL, Sjaastad K, Radomski MW, Volkov Y, Prina-Mello A (2015) Magnetic nanoparticles in cancer theranostics. Theranostics 5:1249
7. Casanovas O (2012) Cancer: Limitations of therapies exposed. Nature 484:44–46
8. Garattini S, Bertele V (2002) Efficacy, safety, and cost of new anticancer drugs. Br Med J 325:269
9. Jain RK (2001) Normalizing tumor vasculature with anti-angiogenic therapy: A new paradigm for combination therapy. Nat Med 7:987–989
10. Van der Seldt AA, Lubberink M, Bahce I, Walraven M, de Boer MP, Greuter HN, Hendrikse NH, Eriksson J, Windhorst AD, Postmus PE, Verheul HM, Serné EH, Lammertsma AA, Smit EF (2012) Rapid decrease in delivery of chemotherapy to tumors after Anti-VEGF therapy: Implications for scheduling of anti-angiogenic drugs. Cancer Cell 21:82–91
11. Sardari D, Verga N (2011) Cancer treatment with hyperthermia. In: Özdemir Ö (ed) Current cancer treatment-novel beyond conventional approaches. InTech, Istanbul, pp 455–475
12. Bush W (1886) Uber den Finfluss wetchen heftigere Eryspelen zuweilen auf organlsierte Neubildungen dusuben. Verh Natruch Preuss Rhein Westphal 23:28–30
13. Jordan A, Scholz R, Wust P, Fähling H, Felix R (1999) Magnetic fluid hyperthermia (MFH): Cancer treatment with AC magnetic field induced excitation of biocompatible superparamagnetic nanoparticles. J. Magn. Magn. Mater. 201:413–419
14. Banobre-López M, Teijeiro A, Rivas J (2013) Magnetic nanoparticle-based hyperthermia for cancer treatment. Rep Practical Oncol Radiother 18:397–400
15. Chichel A, Skowronek J, Kubaszewska M, Kanikowski M (2007) Hyperthermia description of a method and a review of clinical applications. Rep Practical Oncol Radiother 12:267–275
16. Salunkhe AB, Khot VM, Pawar SH (2014) Magnetic hyperthermia with magnetic nanoparticles: a status review. Curr Top Med Chem 14:572–594
17. Wust P, Nadobny J, Fahling H, Riess H, Koch K, John W, Felix R (1991) Determinant factors and disturbances in controlling power distribution patterns by the hyperthermia-ring system BSD-2000. 2. Measuring techniques and analysis. Strahlenther Onkol 167:172–180
18. Andreu I, Natividad E (2013) Accuracy of available methods for quantifying the heat power generation of nanoparticles for magnetic hyperthermia. Int J Hyperthermia 29:739–751
19. Khushrushahi SR (2005) A quantitative design and analysis of magnetic nanoparticle heating systems. Massachusetts Institute of Technology, Cambridge, MA
20. Presman A (2013) Electromagnetic fields and life. Springer, Berlin
21. Cavaliere R, Giogatto BC, Giovanella BC (1967) Selective heat sensitivity of cancer cells. Cancer 20:1351–1381
22. Levine EM, Robbins EB (1970) Differential temperature sensitivity of normal and cancer cells in culture. J Cell Physiol 76:373–379

23. Diederich CJ (2005) Thermal ablation and high-temperature thermal therapy: overview of technology and clinical implementation. Int J Hyperthermia 21:745–753
24. Gneveckow U, Jordan A, Scholz R, Brüss V, Waldöfner N, Ricke J, Feussner A, Hildebrandt B, Rau B, Wust P (2004) Description and characterization of the novel hyperthermia- and thermoablation-system MFH 300F for clinical magnetic fluid hyperthermia. Med Phys 31:1444–1451
25. Dutz S, Hergt R (2013) Magnetic nanoparticle heating and heat transfer on a microscale: basic principles, realities and physical limitations of hyperthermia for tumour therapy. Int J Hyperthermia 29:790–800
26. Valdagni R, Amichetti M (1994) Report of long-term follow-up in a randomized trial comparing radiation therapy and radiation therapy plus hyperthermia to metastatic lymphnodes in stage IV head and neck patients. Int J Radiat Oncol Biol Phys 28:163–169
27. Abdeen S, Praseetha PK (2013) Diagnostics and treatment of metastatic cancers with magnetic nanoparticles. J Nanomedicine Biosci Discov 2013
28. Falk MH, Issels RD (2001) Hyperthermia in oncology. Int J Hyperthermia 17:1–18
29. Jia D, Liu J (2010) Current devices for high-performance whole-body hyperthermia therapy. Expert Rev Med Devices 7:407–423
30. Kim DH, Lee SH, Im KH, Kim KN, Kim KM, Shim IB, Lee MH, Lee YK (2006) Surface-modified magnetite nanoparticles for hyperthermia: Preparation, characterization, and cytotoxicity studies. Curr Appl Phys 6:e242–e246
31. Gilchrist RK, Medal R, Shorey WD, Hanselman RC, Parrott JC, Taylor CB (1957) Selective inductive heating of lymph nodes. Ann Surg 146:596
32. Bai L-Z, Zhao D-L, Xu Y, Zhang J-M, Gao Y-L, Zhao L-Y, Tang J-T (2012) Inductive heating property of graphene oxide-Fe_3O_4 nanoparticles hybrid in an AC magnetic field for localized hyperthermia. Mater Lett 68:399–401
33. Behdadfar B, Kermanpur A, Sadeghi-Aliabadi H, Del Puerto Morales M, Mozaffari M (2012) Synthesis of aqueous ferrofluids of Zn x Fe_3O_4 nanoparticles by citric acid assisted hydrothermal-reduction route for magnetic hyperthermia applications. J. Magn. Magn. Mater. 324:2211–2217
34. Cantillon MP, Wald LL, Zahn M, Adalsteinsson E (2010) Proposing magnetic nanoparticle hyperthermia in low field MRI. Concepts in Magnetic Resonance Part A 36:36–47
35. Fathi Karkan S, Mohammadhosseini M, Panahi Y, Milani M, Zarghami N, Akbarzadeh A, Abasi E, Hosseini A, Davaran S (2016) Magnetic nanoparticles in cancer diagnosis and treatment: a review. Artif Cells Nanomed Biotechnol:1–5
36. Giustini AJ, Petryk AA, Cassim SM, Tate JA, Baker I, Hoopes PI (2010) Magnetic nanoparticle hyperthermia in cancer treatment. Nano Life 1:17–32
37. Goya GF, Grazu V, Ibarra MR (2008) Magnetic nanoparticles for cancer therapy. Current Nanoscience 4:1–16
38. Ito A, Shinkai M, Honda H, Kobayashi T (2005) Medical application of functionalized magnetic nanoparticles. J Biosci Bioeng 100:1–11
39. Pankhurst QA, Connolly J, Jones SK, Dobson JJ (2003) Applications of magnetic nanoparticles in biomedicine. J Phys D Appl Phys 36:R167
40. Choi H, Choi SR, Zhou R, Kung HF, Chen IW (2004) Iron oxide nanoparticles as magnetic resonance contrast agent for tumor imaging via folate receptor-targeted delivery. Acad Radiol 11:996–1004
41. Peng X-H, Qian X, Mao H, Wang AY, Chen ZG, Nie S, Shin DM (2008) Targeted magnetic iron oxide nanoparticles for tumor imaging and therapy. Int J Nanomedicine 3:311–321
42. Jain TK, Richey J, Strand M, Leslie-Pelecky DL, Flask CA, Labhasetwar V (2008) Magnetic nanoparticles with dual functional properties: drug delivery and magnetic resonance imaging. Biomaterials 29:4012–4021
43. Liu X, Chen Y, Li H, Huang N, Jin Q, Ren K, Ji J (2013) Enhanced retention and cellular uptake of nanoparticles in tumors by controlling their aggregation behavior. ACS Nano 7:6244–6257

44. Alonso J, Khurshid H, Devkota J, Nemati Z, Khadka NK, Srikanth H, Pan J, Phan M-H (2016) Superparamagnetic nanoparticles encapsulated in lipid vesicles for advanced magnetic hyperthermia and biodetection. J Appl Phys 119:083904
45. Cervadoro A, Giverso C, Pande R, Sarangi S, Preziosi L, Wosik J, Brazdeikis A, Decuzzi P (2013) Design maps for the hyperthermic treatment of tumors with superparamagnetic nanoparticles. PLoS One 8:e57332
46. Haring M, Schiller J, Mayr J, Grijalvo S, Eritja R, Díaz DD (2015) Magnetic gel composites for hyperthermia cancer therapy. Gels 1:135–161
47. Hoopes PJ, Petryk AA, Gimi B, Giustini AJ, Weaver JB, Bischof J, Chamberlain R, Garwood M (2012) In vivo imaging and quantification of iron oxide nanoparticle uptake and biodistribution. In: SPIE Medical Imaging. International Society for Optics and Photonics, p 83170R-83170R-83179.
48. Stelter L, Pinkernelle JG, Michel R, Schwartlander R, Raschzok N, Morgul MH, Koch M, Denecke T, Ruf J, Baumler H (2010) Modification of aminosilanized superparamagnetic nanoparticles: feasibility of multimodal detection using 3 T MRI, small animal PET, and fluorescence imaging. Mol Imaging Biol 12:25–34
49. Wust P, Gneveckow U, Johannsen M, Böhmer D, Henkel T, Kahmann F, Sehouli J, Felix R (2006) Magnetic nanoparticles for interstitial thermotherapyâ€feasibility, tolerance and achieved temperatures. Int J Hyperthermia 22:673–685
50. Pöttler M, Staicu A, Zaloga J, Unterweger H, Weigel B, Schreiber E, Hofmann S, Wiest I, Jeschke U, Alexiou C (2015) Genotoxicity of superparamagnetic iron oxide nanoparticles in granulosa cells. Int J Mol Sci 16:26280–26290
51. Ahmed M, De Rosales RT, Douek M (2013) Preclinical studies of the role of iron oxide magnetic nanoparticles for nonpalpable lesion localization in breast cancer. J Surg Res 185:27–35
52. Sadhukha T, Wiedmann TS, Panyam J (2013) Inhalable magnetic nanoparticles for targeted hyperthermia in lung cancer therapy. Biomaterials 34:5163–5171
53. Taratula O, Dani RK, Schumann C, Xu H, Wang A, Song H, Dhagat P, Taratula O (2013) Multifunctional nanomedicine platform for concurrent delivery of chemotherapeutic drugs and mild hyperthermia to ovarian cancer cells. Int J Pharm 458:169–180
54. Fortin J-P, Wilhelm C, Servais J, Ménager C, Bacri J-C, Gazeau F (2007) Size-sorted anionic iron oxide nanomagnets as colloidal mediators for magnetic hyperthermia. J Am Chem Soc 129:2628–2635
55. Shreshtha PP, Mohite SS, Jadhav MGK (2015) Review on thermal seeds in magnetic hyperthermia therapy. IJITR 3:2283–2287
56. Hergt R, Andra W, D'ambly CG, Hilger I, Kaiser WA, Richter U, Schmidt HG (1998) Physical limits of hyperthermia using magnetite fine particles. IEEE Trans Magn 34:3745–3754
57. Ramprasad R, Zurcher P, Petras M, Miller M, Renaud P (2004) Magnetic properties of metallic ferromagnetic nanoparticle composites. J Appl Phys 96:519–529
58. Rosensweig RE (2002) Heating magnetic fluid with alternating magnetic field. J. Magn. Magn. Mater. 252:370–374
59. Andra W, Nowak H (2007) Magnetism in medicine: a handbook. Wiley, New York
60. Gubin SP, Koksharov YA, Khomutov GB, Yurkov GVE (2005) Magnetic nanoparticles: preparation, structure and properties. Russ Chem Rev 74:489–520
61. Burrows F, Parker C, Evans RFL, Hancock Y, Hovorka O, Chantrell RW (2010) Energy losses in interacting fine-particle magnetic composites. J Phys D Appl Phys 43:474010
62. Dennis CL, Jackson AJ, Borchers JA, Hoopes PJ, Strawbridge R, Foreman AR, Van Lierop J, Grüttner C, Ivkov R (2009) Nearly complete regression of tumors via collective behavior of magnetic nanoparticles in hyperthermia. Nanotechnology 20:395103
63. Hergt R, Dutz S, Müller R, Zeisberger M (2006) Magnetic particle hyperthermia: nanoparticle magnetism and materials development for cancer therapy. J Phys Condens Matter 18:S2919
64. Hergt R, Dutz S, Röder M (2008) Effects of size distribution on hysteresis losses of magnetic nanoparticles for hyperthermia. J Phys Condens Matter 20:385214

65. Gittleman JI, Abeles B, Bozowski S (1974) Superparamagnetism and relaxation effects in granular Ni-SiO_2 and Ni-Al_2O_3 films. Phys Rev B 9:3891
66. Jordan A, Wust P, Fähling H, John W, Hinz A, Felix R (2009) Inductive heating of ferrimagnetic particles and magnetic fluids: physical evaluation of their potential for hyperthermia. Int J Hyperthermia 25:499–511
67. Lu AH, Salabas EEL, Schüth F (2007) Magnetic nanoparticles: synthesis, protection, functionalization, and application. Angew Chem Int Ed 46:1222–1244
68. Kurti N (1988) Selected works of louis neel. CRC Press, Boca Raton, FL
69. Neel L (1950) Theorie du trainage magnetique des substances massives dans le domaine de Rayleigh. Journal de Physique et le Radium 11:49–61
70. Brown WF Jr (1963) Thermal fluctuations of a single domain particle. J Appl Phys 34: 1319–1320
71. Deissler RJ, Wu Y, Martens MA (2014) Dependence of brownian and neel relaxation times on magnetic field strength. Med Phys 41:012301
72. Lima E Jr, Torres TE, Rossi LM, Rechenberg HR, Berquo TS, Ibarra A, Marquina C, Ibarra MR, Goya GF (2013) Size dependence of the magnetic relaxation and specific power absorption in iron oxide nanoparticles. J Nanopart Res 15:1–11
73. Zhang X, Chen S, Wang H-M, Hsieh S-L, Wu C-H, Chou H-H, Hsieh S (2010) Role of neel and brownian relaxation mechanisms for water-based Fe_3O_4 nanoparticle ferrofluids in hyperthermia. Biomed Eng: Appl Basis Commun 22:393–399
74. Motoyama J, Hakata T, Kato R, Yamashita N, Morino T, Kobayashi T, Honda H (2010) Size dependent heat generation of magnetic nanoparticles under AC magnetic field for cancer therapy. In: Animal cell technology: Basic & applied aspects. Springer, pp 415–421
75. Guibert CM, Dupuis V, Peyre V, Fresnais JRM (2015) Hyperthermia of magnetic nanoparticles: experimental study of the role of aggregation. J Phys Chem C 119:28148–28154
76. Obaidat IM, Issa B, Haik Y (2015) Magnetic properties of magnetic nanoparticles for efficient hyperthermia. Nanomaterials 5:63–89
77. Thanh NTK (2012) Magnetic nanoparticles: from fabrication to clinical applications. CRC press, Boca Raton, FL
78. Yahya N (2011) Carbon and oxide nanostructures: synthesis, characterisation and applications. Springer, Berlin
79. Basti H, Hanini A, Levy M, Tahar LB, Herbst F, Smiri LS, Kacem K, Gavard J, Wilhelm C, Gazeau F (2014) Size tuned polyol-made $Zn_{0.9}M_{0.1}Fe_2O_4$ (M=Mn, Co, Ni) ferrite nanoparticles as potential heating agents for magnetic hyperthermia: from synthesis control to toxicity survey. Mater Res Exp 1:045047
80. Beji Z, Hanini A, Smiri LS, Gavard J, Kacem K, Villain F, Grenèche JM, Chau F, Ammar S (2010) Magnetic properties of Zn-substituted $MnFe_2O_4$ nanoparticles synthesized in polyol as potential heating agents for hyperthermia. Evaluation of their toxicity on Endothelial cells. Chem Mater 22:5420–5429
81. Cespedes E, Byrne JM, Farrow N, Moise S, Coker VS, Bencsik M, Lloyd JR, Telling ND (2014) Bacterially synthesized ferrite nanoparticles for magnetic hyperthermia applications. Nanoscale 6:12958–12970
82. Hanini A, Lartigue L, Gavard J, Schmitt A, Kacem K, Wilhelm C, Gazeau F, Chau F, Ammar S (2016) Thermosensitivity profile of malignant glioma U87-MG cells and human endothelial cells following $\hat{I}^3$-Fe_2O_3 NPs internalization and magnetic field application. RSC Advances 6:15415–15423
83. Lin M, Huang J, Sha M (2014) Recent advances in nanosized Mn-Zn ferrite magnetic fluid hyperthermia for cancer treatment. J Nanosci Nanotechnol 14:792–802
84. Veverka M, Zăväta K, Kaman O, Veverka P, Knížek K, Pollert E, Burian M, Kašpar P (2014) Magnetic heating by silica-coated Co-Zn ferrite particles. J Phys D Appl Phys 47:065503
85. Hanini A, Lartigue L, Gavard J, Kacem K, Wilhelm C, Gazeau F, Chau FO, Ammar S (2016) Zinc substituted ferrite nanoparticles with $Zn_{0.9}Fe_{2.1}O_4$ formula used as heating agents for in vitro hyperthermia assay on glioma cells. J. Magn. Magn. Mater. 416:315–320

86. Wijaya A, Brown KA, Alper JD, Hamad-Schifferli K (2007) Magnetic field heating study of Fe-doped Au nanoparticles. J Magn Magn Mater 309:15–19
87. Hilger I, Kaiser WA (2012) Iron oxide-based nanostructures for MRI and magnetic hyperthermia. Nanomedicine 7:1443–1459
88. Neuberger T, Schöpf B, Hofmann H, Hofmann M, Von Rechenberg B (2005) Superparamagnetic nanoparticles for biomedical applications: possibilities and limitations of a new drug delivery system. J. Magn. Magn. Mater. 293:483–496
89. Hiergeist R, Andrã W, Buske N, Hergt R, Hilger I, Richter U, Kaiser W (1999) Application of magnetite ferrofluids for hyperthermia. J Magn Magn Mater 201:420–422
90. Gonzales-Weimuller M, Zeisberger M, Krishnan KM (2009) Size-dependant heating rates of iron oxide nanoparticles for magnetic fluid hyperthermia. J. Magn. Magn. Mater. 321: 1947–1950
91. Guardia P, Di Corato R, Lartigue L, Wilhelm C, Espinosa A, Garcia-Hernandez M, Gazeau F, Manna L, Pellegrino T (2012) Water-soluble iron oxide nanocubes with high values of specific absorption rate for cancer cell hyperthermia treatment. ACS Nano 6:3080–3091
92. Lartigue LN, Hugounenq P, Alloyeau D, Clarke SP, Lévy M, Bacri J-C, Bazzi R, Brougham DF, Wilhelm C, Gazeau F (2012) Cooperative organization in iron oxide multi-core nanoparticles potentiates their efficiency as heating mediators and MRI contrast agents. ACS Nano 6:10935–10949
93. Kolosnjaj-Tabi J, Di Corato R, Lartigue LN, Marangon I, Guardia P, Silva AKA, Luciani N, Clément O, Flaud P, Singh JV (2014) Heat-generating iron oxide nanocubes: subtle "destructurators" of the tumoral microenvironment. ACS Nano 8:4268–4283
94. Di Corato R, Espinosa A, Lartigue L, Tharaud M, Chat S, Pellegrino T, Ménager C, Gazeau F, Wilhelm C (2014) Magnetic hyperthermia efficiency in the cellular environment for different nanoparticle designs. Biomaterials 35:6400–6411
95. Gandhi S, Arami H, Krishnan KM (2016) Detection of cancer-specific proteases using magnetic relaxation of peptide-conjugated nanoparticles in biological environment. Nano Lett
96. Lowry GV, Gregory KB, Apte SS, Lead JR (2012) Transformations of nanomaterials in the environment. Environ Sci Technol 46:6893–6899
97. Thomas CR, George S, Horst AM, Ji Z, Miller RJ, Peralta-Videa JR, Xia T, Pokhrel S, Maìdler L, Gardea-Torresdey JL (2011) Nanomaterials in the environment: from materials to high-throughput screening to organisms. ACS Nano 5:13–20
98. Levard C, Hotze EM, Lowry GV, Brown GE Jr (2012) Environmental transformations of silver nanoparticles: impact on stability and toxicity. Environ Sci Technol 46:6900–6914
99. Xia T, Zhao Y, Sager T, George S, Pokhrel S, Li N, Schoenfeld D, Meng H, Lin S, Wang X (2011) Decreased dissolution of ZnO by iron doping yields nanoparticles with reduced toxicity in the rodent lung and zebrafish embryos. ACS Nano 5:1223–1235
100. Kolosnjaj-Tabi J, Lartigue LN, Javed Y, Luciani N, Pellegrino T, Wilhelm C, Alloyeau D, Gazeau F (2016) Biotransformations of magnetic nanoparticles in the body. Nano Today 11:280–284
101. Koksharov YA (2009) Magnetism of nanoparticles: Effects of size, shape, and interactions. In: Gubin SP (ed) Magnetic nanoparticles. Wiley-VCH, pp 197–254
102. Alloyeau D, Dachraoui W, Javed Y, Belkahla H, Wang G, Lecoq HLN, Ammar S, Ersen O, Wisnet A, Gazeau F (2015) Unravelling kinetic and thermodynamic effects on the growth of gold nanoplates by liquid transmission electron microscopy. Nano Lett 15:2574–2581
103. Laurent S, Dutz S, Häfeli UO, Mahmoudi M (2011) Magnetic fluid hyperthermia: focus on superparamagnetic iron oxide nanoparticles. Adv Colloid Interface Sci 166:8–23
104. Chen D, Xu R (1998) Hydrothermal synthesis and characterization of nanocrystalline Fe_3O_4 powders. Mater Res Bull 33:1015–1021
105. Lawrence MJ, Rees GD (2000) Microemulsion-based media as novel drug delivery systems. Adv Drug Deliv Rev 45:89–121
106. Titirici M-M, Antonietti M, Thomas A (2006) A generalized synthesis of metal oxide hollow spheres using a hydrothermal approach. Chem Mater 18:3808–3812

107. Cheng C, Xu F, Gu H (2011) Facile synthesis and morphology evolution of magnetic iron oxide nanoparticles in different polyol processes. New J Chem 35:1072–1079
108. Laurent S, Forge D, Port M, Roch A, Robic C, Vander Elst L, Muller RN (2008) Magnetic iron oxide nanoparticles: synthesis, stabilization, vectorization, physicochemical characterizations, and biological applications. Chem Rev 108:2064–2110
109. Hoskins C, Min Y, Gueorguieva M, Mcdougall C, Volovick A, Prentice P, Wang Z, Melzer A, Cuschieri A, Wang L (2012) Hybrid gold-iron oxide nanoparticles as a multifunctional platform for biomedical application. J Nanobiotechnol 10:1
110. Gao J, Gu H, Xu B (2009) Multifunctional magnetic nanoparticles: design, synthesis, and biomedical applications. Acc Chem Res 42:1097–1107
111. Salvador-Morales C, Gao W, Ghatalia P, Murshed F, Aizu W, Langer R, Farokhzad OC (2009) Multifunctional nanoparticles for prostate cancer therapy. Expert Rev Anticancer Ther 9: 211–221
112. Bergey EJ, Levy L, Wang X, Krebs LJ, Lal M, Kim K-S, Pakatchi S, Liebow C, Prasad PN (2002) DC magnetic field induced magnetocytolysis of cancer cells targeted by LH-RH magnetic nanoparticles in vitro. Biomed Microdevices 4:293–299
113. Berry CC, Curtis ASG (2003) Functionalisation of magnetic nanoparticles for applications in biomedicine. J Phys D Appl Phys 36:R198
114. Briley-Saebo KC, Johansson LO, Hustvedt SO, Haldorsen AG, Bjørnerud A, Fayad ZA, Ahlstrom HK (2006) Clearance of iron oxide particles in rat liver: effect of hydrated particle size and coating material on liver metabolism. Invest Radiol 41:560–571
115. Kolosnjaj-Tabi J, Javed Y, Lartigue LN, Volatron J, Elgrabli D, Marangon I, Pugliese G, Caron B, Figuerola A, Luciani N (2015) The one year fate of iron oxide coated gold nanoparticles in mice. ACS Nano 9:7925–7939
116. Levy M, Luciani N, Alloyeau D, Elgrabli D, Deveaux V, Pechoux C, Chat S, Wang G, Vats N, Gendron FO (2011) Long term in vivo biotransformation of iron oxide nanoparticles. Biomaterials 32:3988–3999
117. Mahmoudi M, Lynch I, Ejtehadi MR, Monopoli MP, Bombelli FB, Laurent S (2011) Protein nanoparticle interactions: opportunities and challenges. Chem Rev 111:5610–5637
118. Sperling RA, Parak WJ (2010) Surface modification, functionalization and bioconjugation of colloidal inorganic nanoparticles. Philos Trans R Soc Lond A: Math Phys Eng Sci 368: 1333–1383
119. Lazzari S, Moscatelli D, Codari F, Salmona M, Morbidelli M, Diomede L (2012) Colloidal stability of polymeric nanoparticles in biological fluids. J Nanopart Res 14:1–10
120. Ditto AJ, Shah KN, Robishaw NK, Panzner MJ, Youngs WJ, Yun YH (2012) The Interactions between l-tyrosine based nanoparticles decorated with folic acid and cervical cancer cells under physiological flow. Mol Pharm 9:3089–3098
121. Kumar S, Aaron J, Sokolov K (2008) Directional conjugation of antibodies to nanoparticles for synthesis of multiplexed optical contrast agents with both delivery and targeting moieties. Nat Protoc 3:314–320
122. Gupta AK, Gupta M (2005) Synthesis and surface engineering of iron oxide nanoparticles for biomedical applications. Biomaterials 26:3995–4021
123. Sperling RA, Gil PR, Zhang F, Zanella M, Parak WJ (2008) Biological applications of gold nanoparticles. Chem Soc Rev 37:1896–1908
124. Mohammad F, Balaji G, Weber A, Uppu RM, Kumar CSSR (2010) Influence of gold nanoshell on hyperthermia of superparamagnetic iron oxide nanoparticles. J Phys Chem C 114:19194–19201
125. Javed Y, Lartigue LN, Hugounenq P, Vuong QL, Gossuin Y, Bazzi R, Wilhelm C, Ricolleau C, Gazeau F, Alloyeau D (2014) Biodegradation mechanisms of iron oxide monocrystalline nanoflowers and tunable shield effect of gold coating. Small 10:3325–3337
126. Li S-D, Huang L (2008) Pharmacokinetics and biodistribution of nanoparticles. Mol Pharm 5:496–504
127. Owens DE, Peppas NA (2006) Opsonization, biodistribution, and pharmacokinetics of polymeric nanoparticles. Int J Pharm 307:93–102

128. Shilo M, Sharon A, Baranes K, Motiei M, Lellouche J-PM, Popovtzer R (2015) The effect of nanoparticle size on the probability to cross the blood-brain barrier: an in-vitro endothelial cell model. J Nanobiotechnol 13:1
129. Longmire M, Choyke PL, Kobayashi H (2008) Clearance properties of nano-sized particles and molecules as imaging agents: considerations and caveats.
130. Alexis F, Pridgen E, Molnar LK, Farokhzad OC (2008) Factors affecting the clearance and biodistribution of polymeric nanoparticles. Mol Pharm 5:505–515
131. Czuprynski CJ (2016) Opsonization and Phagocytosis. Encyclopedia of Immunotoxicology: 674–676
132. Salmaso S, Caliceti P (2013) Stealth properties to improve therapeutic efficacy of drug nanocarriers. J Drug Deliv 2013:19
133. Al-Hanbali O, Rutt KJ, Sarker DK, Hunter AC, Moghimi SM (2006) Concentration dependent structural ordering of poloxamine 908 on polystyrene nanoparticles and their modulatory role on complement consumption. J Nanosci Nanotechnol 6:3126–3133
134. Jo DH, Kim JH, Lee TG, Kim JH (2015) Size, surface charge, and shape determine therapeutic effects of nanoparticles on brain and retinal diseases. Nanomed: Nanotechnol, Biol Med 11:1603–1611
135. Frohlich E (2012) The role of surface charge in cellular uptake and cytotoxicity of medical nanoparticles. Int J Nanomedicine 7:5577–5591
136. Rahman M, Laurent S, Tawil N, Yahia LH, Mahmoudi M (2013) Nanoparticle and protein corona. In: Protein-nanoparticle interactions. Springer, pp 21–44
137. Dell'orco D, Lundqvist M, Oslakovic C, Cedervall T, Linse S (2010) Modeling the time evolution of the nanoparticle-protein corona in a body fluid. PLoS One 5:e10949
138. Bargheer D, Nielsen J, Gébel G, Heine M, Salmen SC, Stauber R, Weller H, Heeren J, Nielsen P (2015) The fate of a designed protein corona on nanoparticles in vitro and in vivo. Beilstein J Nanotechnol 6:36–46
139. Foroozandeh P, Aziz AA (2015) Merging worlds of nanomaterials and biological environment: factors governing protein corona formation on nanoparticles and its biological consequences. Nanoscale Res Lett 10:1–12
140. Medina C, Santos-Martinez MJ, Radomski A, Corrigan OI, Radomski MW (2007) Nanoparticles: pharmacological and toxicological significance. Br J Pharmacol 150:552–558
141. Shang L, Nienhaus K, Nienhaus GU (2014) Engineered nanoparticles interacting with cells: size matters. J Nanobiotechnol 12:1
142. Cummings BS, Wills LP, Schnellmann RG (2012) Measurement of cell death in Mammalian cells. Current Protocols in Pharmacology 12.18. 11–12.18. 24.
143. Naqvi S, Samim M, Abdin M, Ahmed FJ, Maitra A, Prashant C, Dinda AK (2009) Concentration-dependent toxicity of iron oxide nanoparticles mediated by increased oxidative stress. Int J Nanomedicine 5:983–989
144. Ghosh R, Pradhan L, Devi YP, Meena SS, Tewari R, Kumar A, Sharma S, Gajbhiye NS, Vatsa RK, Pandey BN (2011) Induction heating studies of Fe_3O_4 magnetic nanoparticles capped with oleic acid and polyethylene glycol for hyperthermia. J Mater Chem 21:13388–13398
145. Ma M, Wu Y, Zhou J, Sun Y, Zhang Y, Gu N (2004) Size dependence of specific power absorption of Fe_3O_4 particles in AC magnetic field. J. Magn. Magn. Mater. 268:33–39
146. Zhao D-L, Wang X-X, Zeng X-W, Xia Q-S, Tang J-T (2009) Preparation and inductive heating property of Fe_3O_4 chitosan composite nanoparticles in an AC magnetic field for localized hyperthermia. J Alloys Compd 477:739–743
147. Sadat ME, Patel R, Sookoor J, Bud'ko SL, Ewing RC, Zhang J, Xu H, Wang Y, Pauletti GM, Mast DB (2014) Effect of spatial confinement on magnetic hyperthermia via dipolar interactions in Fe_3O_4 nanoparticles for biomedical applications. Mater Sci Eng C 42:52–63
148. Kozissnik B, Bohorquez AC, Dobson J, Rinaldi C (2013) Magnetic fluid hyperthermia: Advances, challenges, and opportunity. Int J Hyperthermia 29:706–714
149. Fadeel B, Garcia-Bennett AE (2010) Better safe than sorry: Understanding the toxicological properties of inorganic nanoparticles manufactured for biomedical applications. Adv Drug Deliv Rev 62:362–374

150. Kida Y, Ishiguri H, Ichimi K, Kobayashi T (1990) Hyperthermia of metastatic brain tumor with implant heating system: a preliminary clinical results. No shinkei geka. Neurol Surg 18:521–526
151. Kobayashi T, Kida Y, Matsui M, Amemiya Y (1990) Interstitial hyperthermia of malignant brain tumors using implant heating system (IHS). No shinkei geka. Neurol Surg 18:247–252
152. Luo S, Wang LF, Ding WJ, Wang H, Zhou JM, Jin HK, Su SF, Ouyang WW (2014) Clinical trials of magnetic induction hyperthermia for treatment of tumours. OA Cancer 2:2
153. Hentschel M, Mirtsch S, Jordan A, Wust P, Vogl TH, Semmler W, Wolf KJ, Felix R (1997) Heat response of HT29 cells depends strongly on perfusion–A 31P NMR spectroscopy, HPLC and cell survival analysis. Int J Hyperthermia 13:69–82
154. Maier-Hauff K, Rothe R, Scholz R, Gneveckow U, Wust P, Thiesen B, Feussner A, Von Deimling A, Waldoefner N, Felix R (2007) Intracranial thermotherapy using magnetic nanoparticles combined with external beam radiotherapy: results of a feasibility study on patients with glioblastoma multiforme. J Neurooncol 81:53–60
155. Maier-Hauff K, Ulrich F, Nestler D, Niehoff H, Wust P, Thiesen B, Orawa H, Budach V, Jordan A (2011) Efficacy and safety of intratumoral thermotherapy using magnetic iron-oxide nanoparticles combined with external beam radiotherapy on patients with recurrent glioblastoma multiforme. J Neurooncol 103:317–324
156. Johannsen M, Gneveckow U, Thiesen B, Taymoorian K, Cho CH, Waldöfner N, Scholz R, Jordan A, Loening SA, Wust P (2007) Thermotherapy of prostate cancer using magnetic nanoparticles: Feasibility, imaging, and three-dimensional temperature distribution. Eur Urol 52:1653–1662
157. Gao F, Yan Z, Zhou J, Cai Y, Tang J (2012) Methotrexate-conjugated magnetic nanoparticles for thermochemotherapy and magnetic resonance imaging of tumor. J Nanopart Res 14:1–10